



# X-ray Detectors for Synchrotrons



3rd EIROforum School on Instrumentation  
27-31 May 2013

J Morse\*  
Detector Unit, Instrument Services and Development Division  
European Synchrotron Radiation Facility, Grenoble.

*\*with thanks for contributions from P Fajardo- Th Martin- C. Ponchut- ESRF & H. Graafsma-DESY*

1. 3rd Generation synchrotron sources: a (very) quick introduction
2. what are we trying to measure?
3. different experimental methods, and some of the major detectors in use
  - all dosed with a little bit of basic X-ray and detector physics.



European Synchrotron  
Radiation Facility

50 beamlines in operation

7000 external users / year

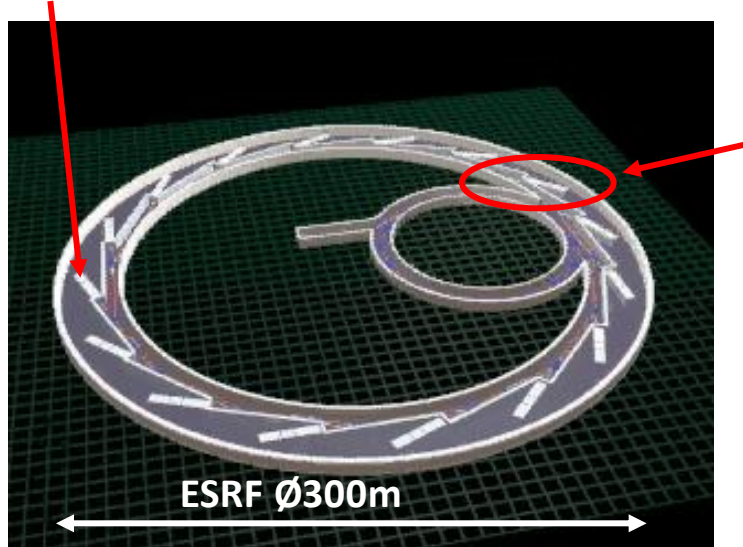
high intensity, semi-coherent X-ray beams  
~0.5keV – 0.5MeV for diffraction and  
inelastic scattering studies

basic and applied research in:

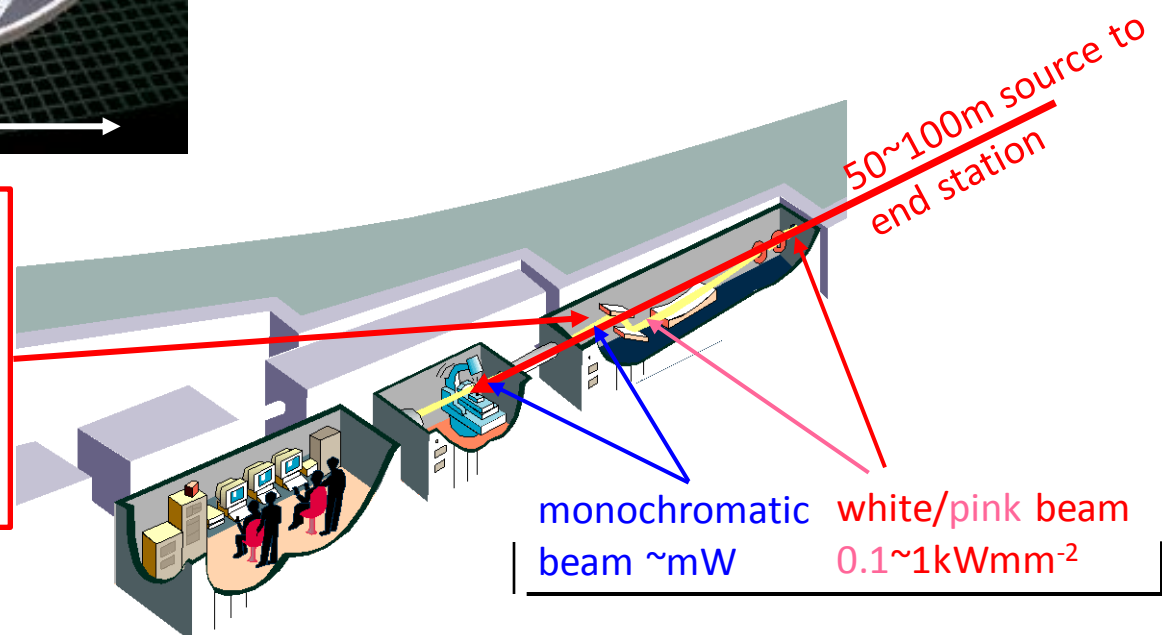
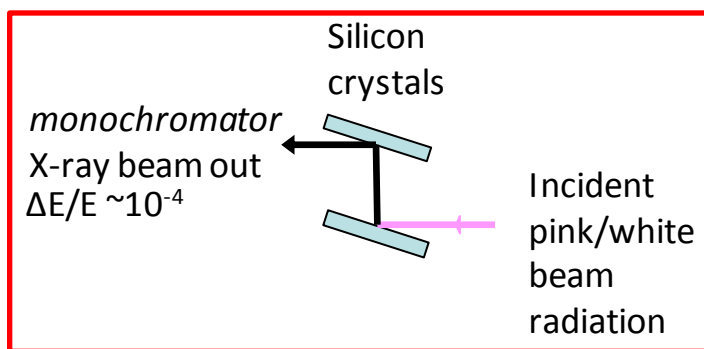
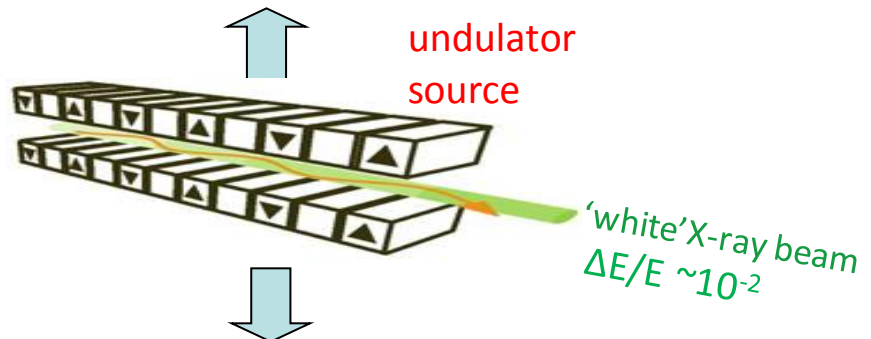
biology (e.g. protein structures...)  
materials science  
chemistry & catalysis...  
2D- & 3D (coherent, diffractive...) imaging  
archaeology-paleontology  
...

-- at molecular & atomic scales...

~ 50 beamlines



energy tunability



beam *at the sample*

Size:	- Unfocused beam:	few millimeters to a few cm (source is divergent)
	- Focused beam:	<100 nanometers to 10's of microns
Energy range:		<0.5 keV to 0.5MeV, but mostly 3 ... 100keV
Energy bandwidth ( $\Delta E/E$ ):		$10^{-2}$ to $10^{-8}$ at sample, typically $\Delta E \sim$ few eV @ 20keV
Photon flux (@ $\Delta E/E = 10^{-4}$ ):		$10^9 - 10^{14}$ ph/sec ('online' attenuators )

*but extremely variable photon rates incident on the detector(s)*

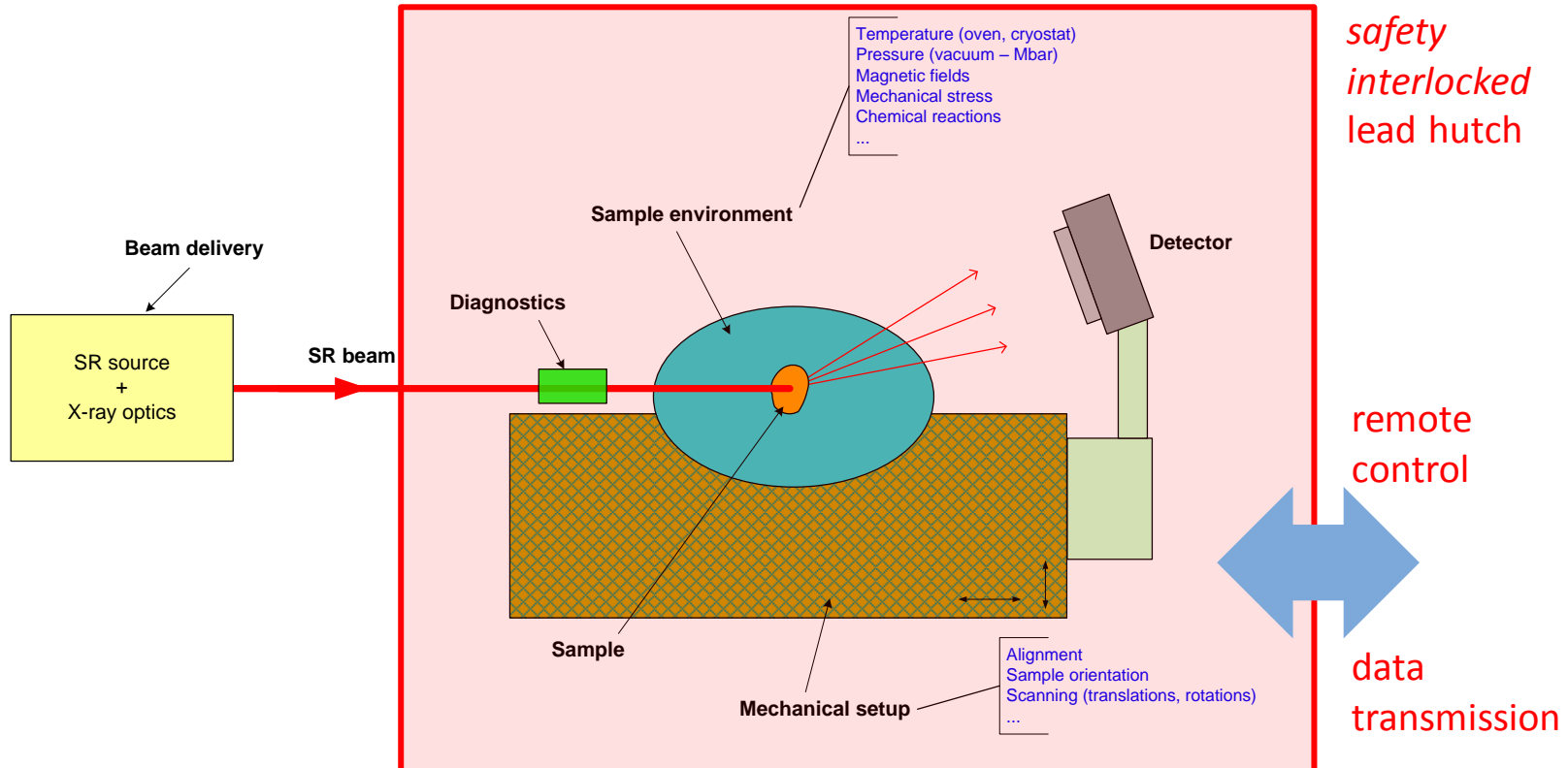
from <1 photon /sec up to 'near full beam' flux

*nb. X-ray ionizing radiation dose = sample damage !*

e.g. at  $10^{12}$  ph/s and 10 keV photons , *dose rate*  $\sim 10$  Gray/sec in a silicon

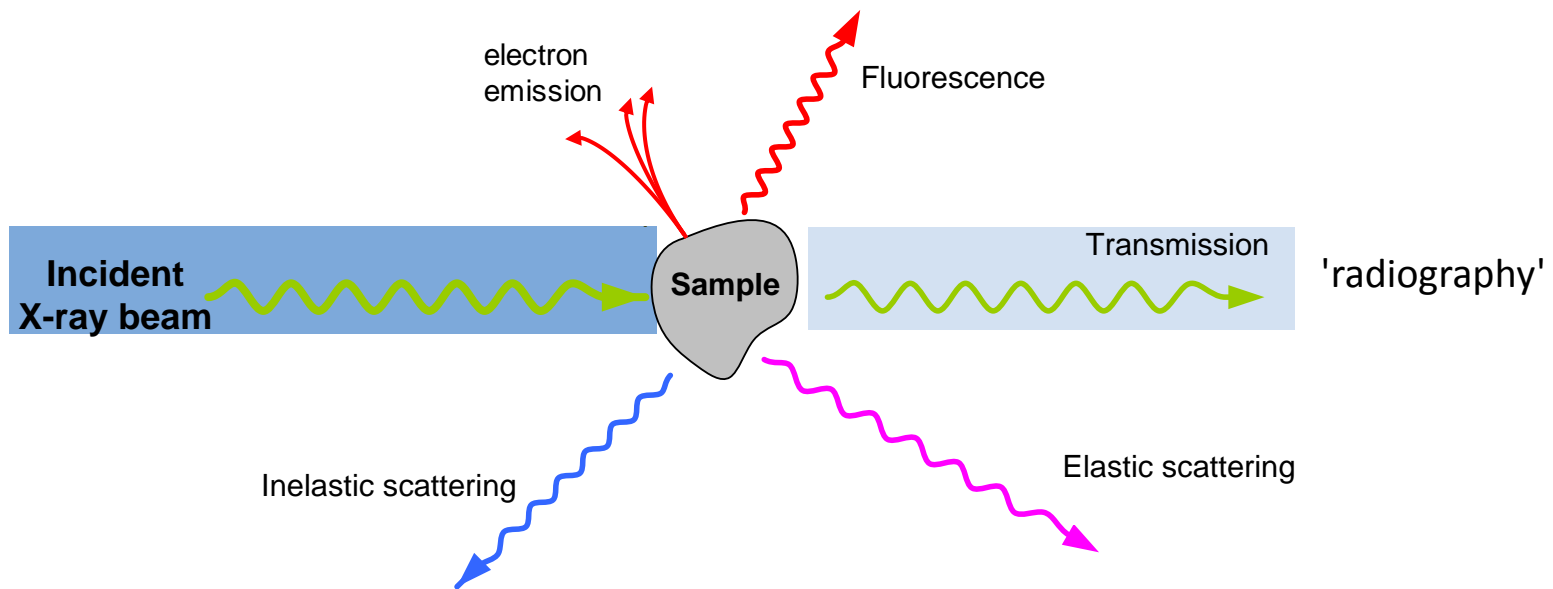
*experiments are built around the samples to be measured*

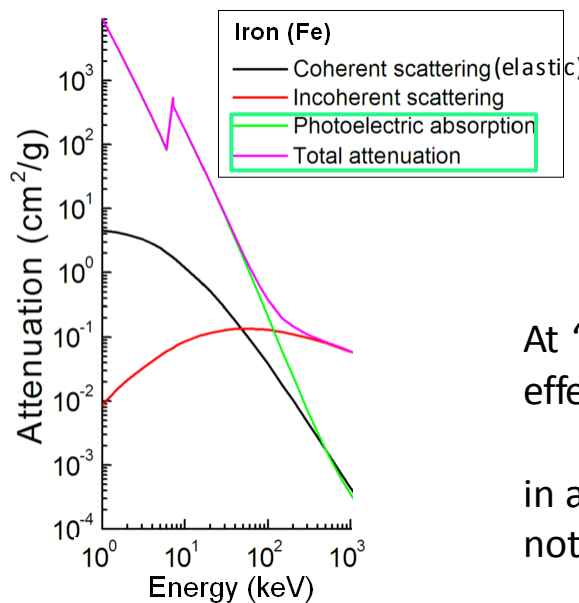
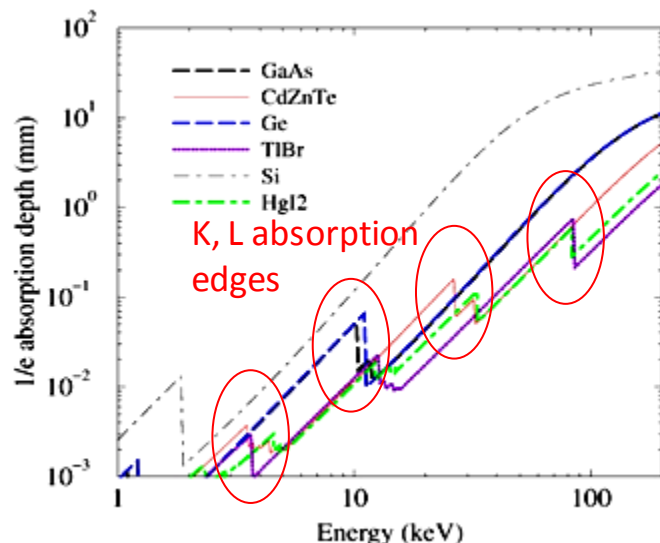
--> importance of sample environment (temperature; pressure; E and B fields...)  
need to physically manipulate sample during measurements (position, rotation...)



*rapid turnover of samples and experiments*

sample(s) in beam for minutes to hours  
experiments typically lasts a few days





*Beer's law:*

$$I(x) = I_0 \exp(-\mu(E) \cdot x)$$

intensity of a photon beam decreases exponentially with distance into the material,

*but the energy of photons in the transmitted beam remains the same.*

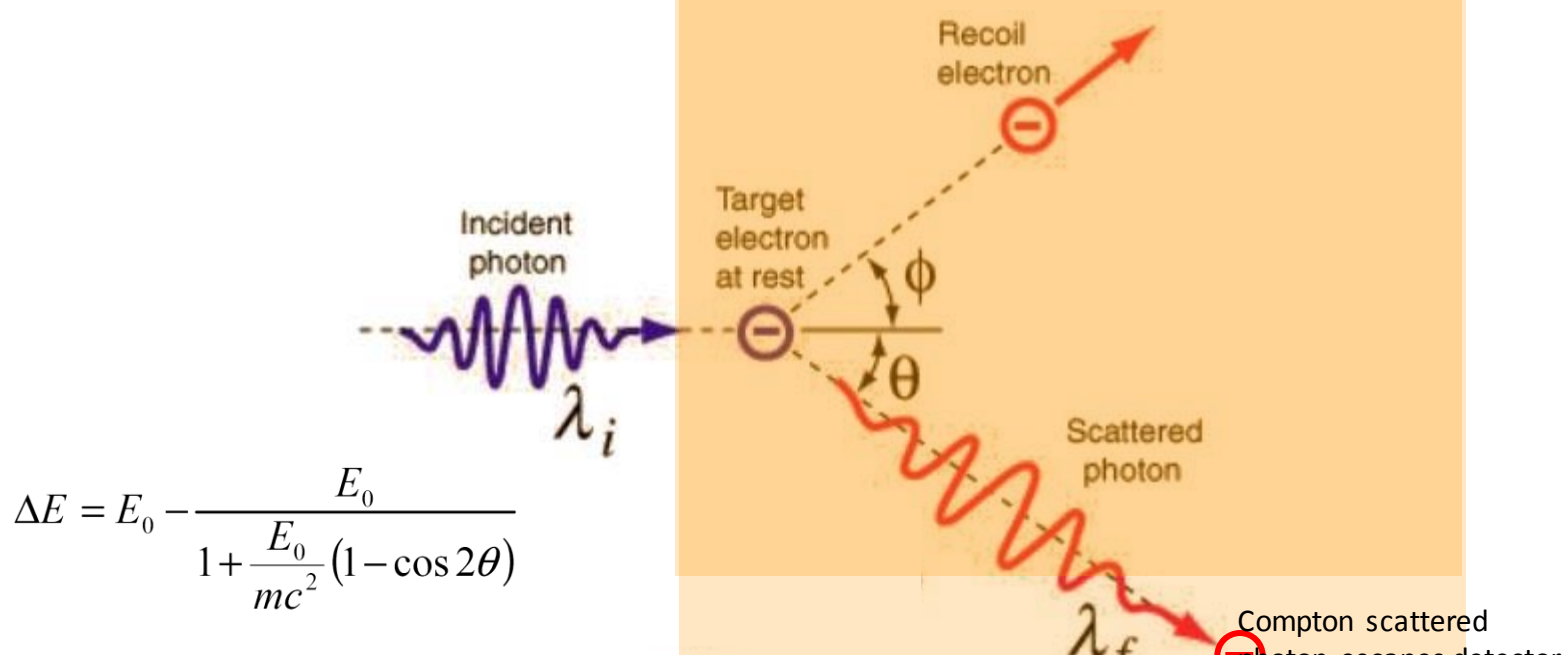
note that  $\mu(E)$  is discontinuous at 'absorption edge' energies, corresponding to the atomic shell structure binding energies

At 'low' synchrotron energies, the photoelectric effect is usually the dominant interaction

in a detector, incoherent (Compton) scattering is not desirable...

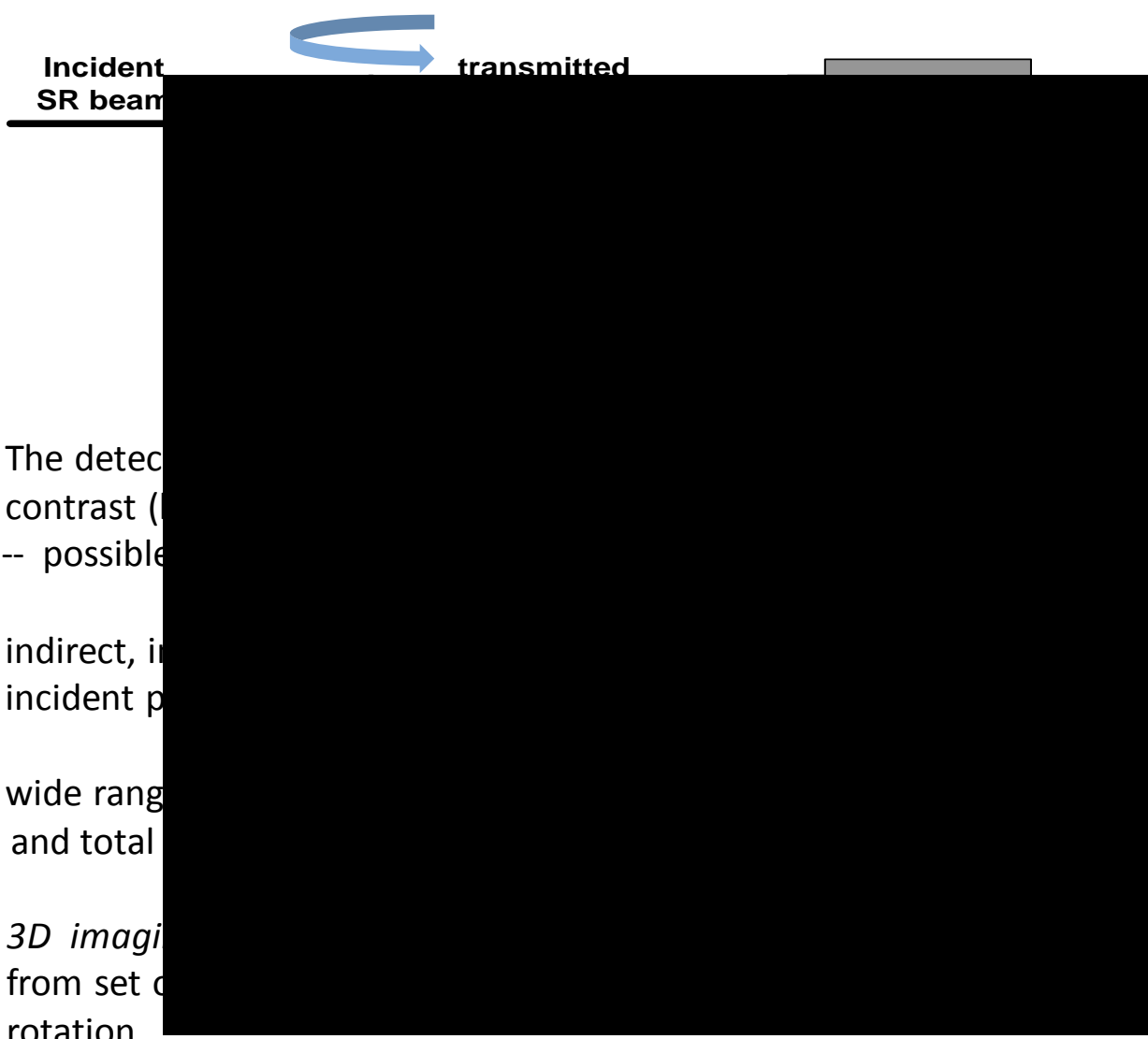
$$\Delta E = E_0 - \frac{E_0}{1 + \frac{E_0}{mc^2}(1 - \cos 2\theta)}$$

and  $E = hc/\lambda$



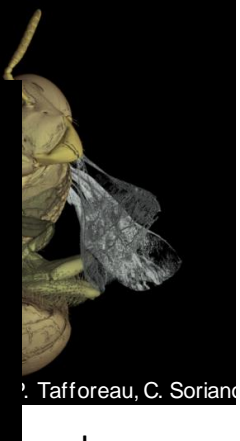
The diagram illustrates the Compton scattering process within a 'Detector Material' represented by a large orange rectangle. An 'Incident photon' (purple wavy line) with wavelength  $\lambda_i$  strikes a 'Target electron at rest' (black circle with a minus sign). The electron scatters a 'Scattered photon' (red wavy line) with wavelength  $\lambda_f$ . The angle between the incident and scattered photons is  $2\theta$ , and the angle between the target electron's initial direction and its recoil path is  $\phi$ . A red circle with a minus sign highlights the 'Scattered photon escapes detector' path, which is labeled 'photoelectric absorption'.

X! measured energy Compton scattered electron only Compton photon)



- The detection scheme can provide high contrast (good SNR)
  - possible to image live specimens
- indirect, inelastic scattering
  - incident particle energy
- wide range of scattering angles and total intensity
- *3D imaging* by combining images from set of projections over a rotation

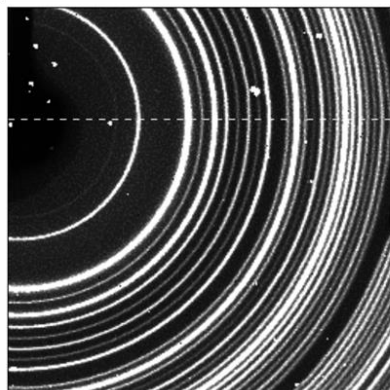
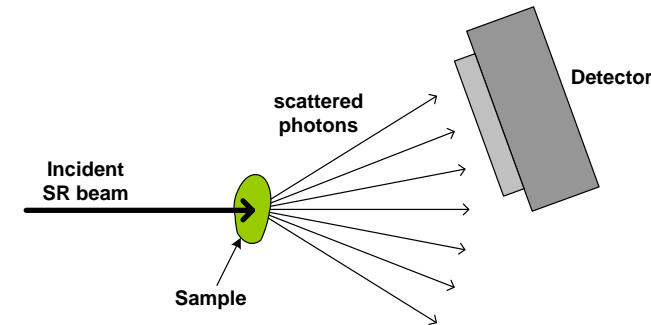
Paul Tafforeau, ESRF



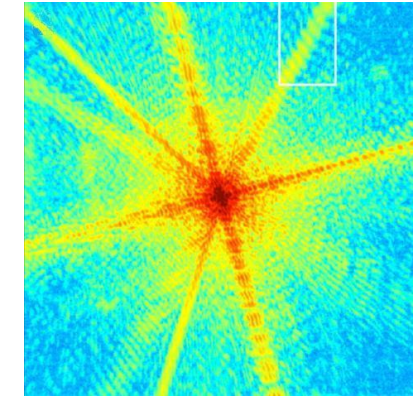
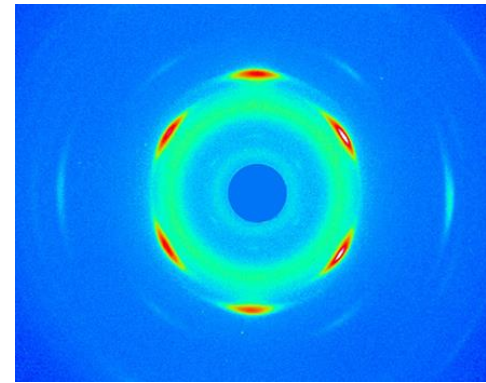
• The detection scheme  
can provide high contrast (good SNR)  
-- possible to image live specimens



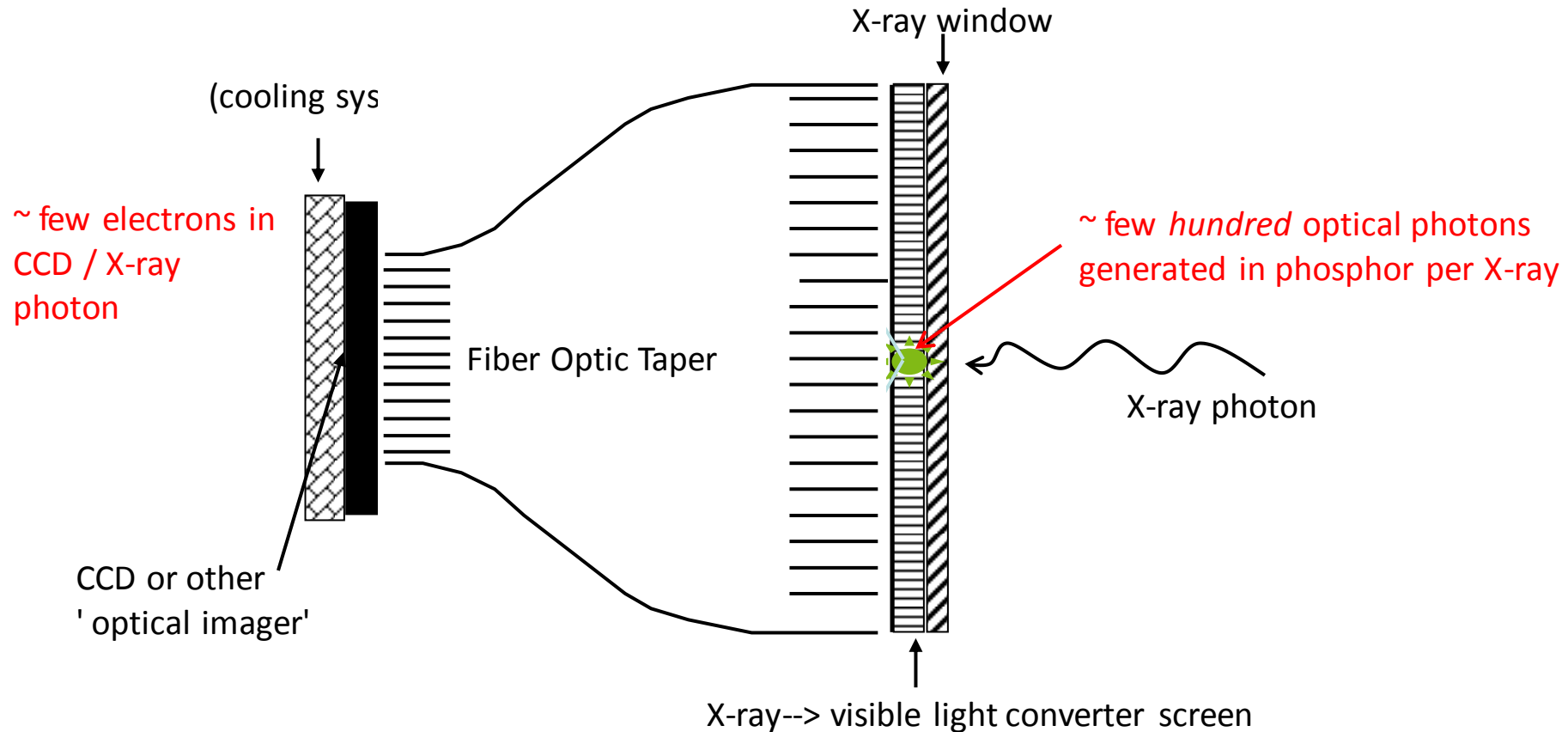
- Scattered photons *conserve their initial energy*, i.e. only momentum changed  
*angular measurements* are required, usually measured with 2D spatially resolving detectors
  - > angular resolution can be varied with changing detector-sample distance
- Large dynamic range may be required (crystal diffraction can cover ~8 orders of magnitude!)
- detectors used:
  - scintillator-PMT; silicon-diode, -APD using diffractometer
  - solid state semiconductors (1D strip, **2D area PADs**)
  - 'indirect detection' with flat panel a-Si or CMOS readout  
**2D area scintillator-optic-CCD cameras**  
(laser read-out phosphor image plates, MWPC gas detectors)



1e4  
2.0  
1.8  
1.6  
1.4  
1.2  
1.0  
0.8  
0.6  
0.4  
0.2  
0.0

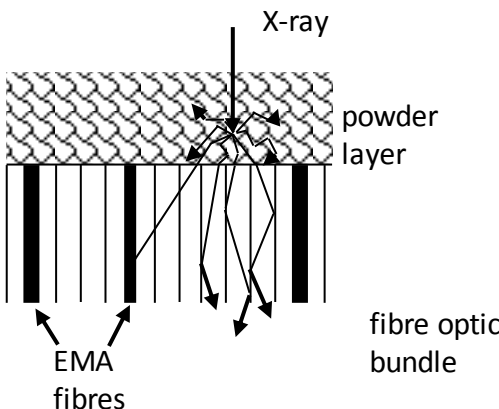


position-resolved 2D area detectors, especially high resolution X-ray imaging

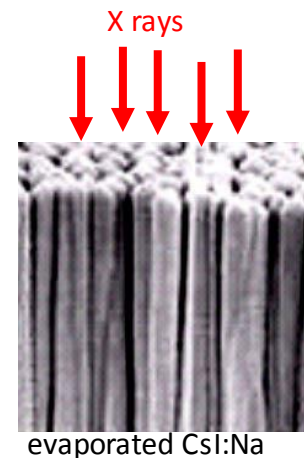


for detector areas above  $\sim 1\text{cm}^2$ , fibre optic gives more efficient optical coupling to CCD

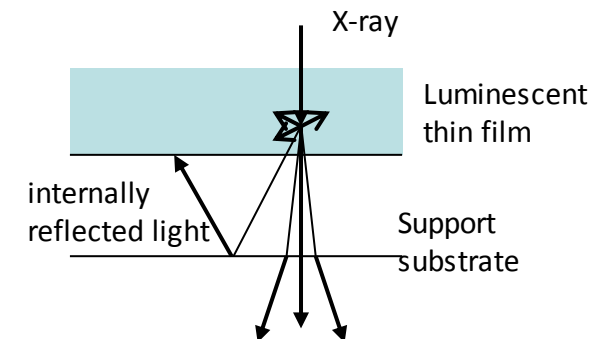
powdered crystal  
'phosphor' screen



structured crystal growth  
scintillator



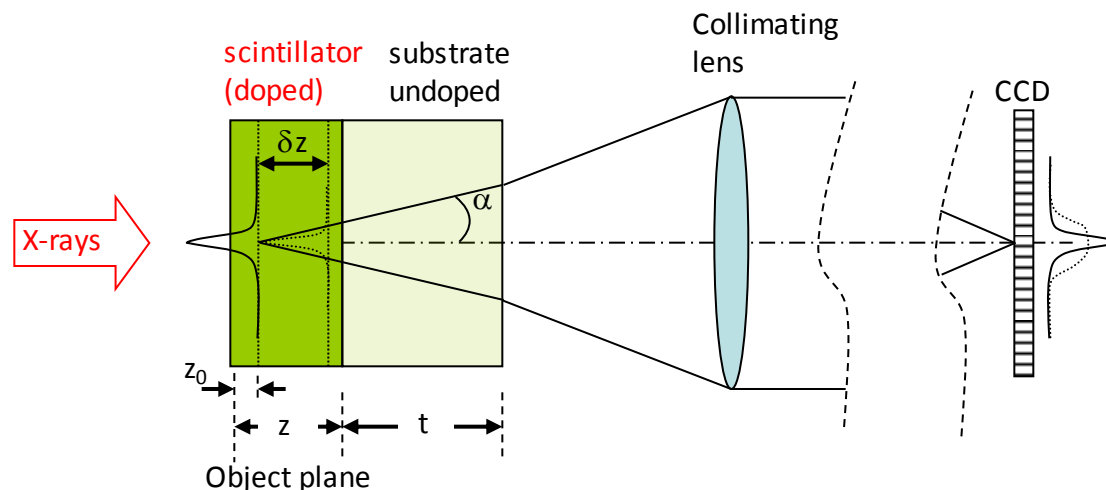
single crystal screen



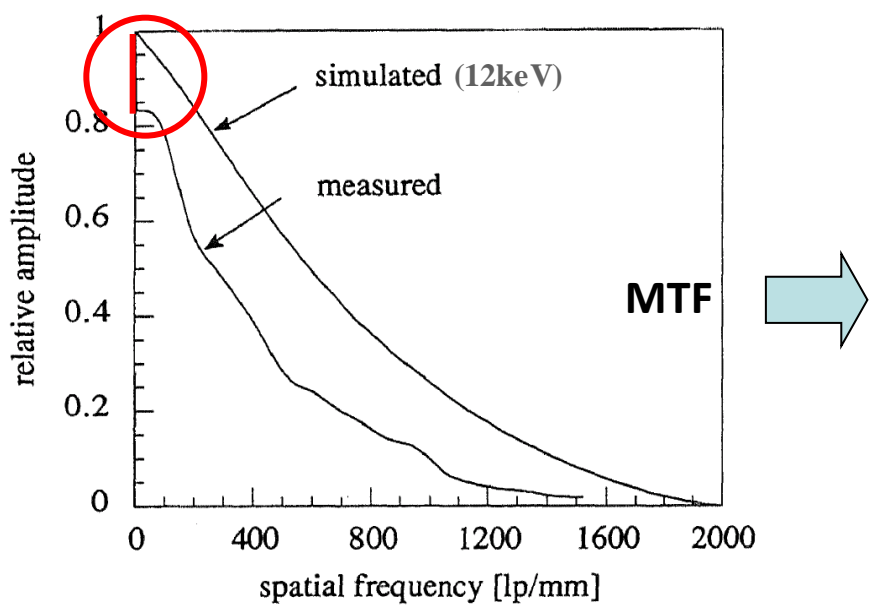
Spatial resolution limit  $\sim 5\mu\text{m}$  fwhm  
median particle sizes (P43 'Gadox')  
 $2.5\mu\text{m}$  to  $30\mu\text{m}$

need for encapsulation  
(fragile, hygroscopic)

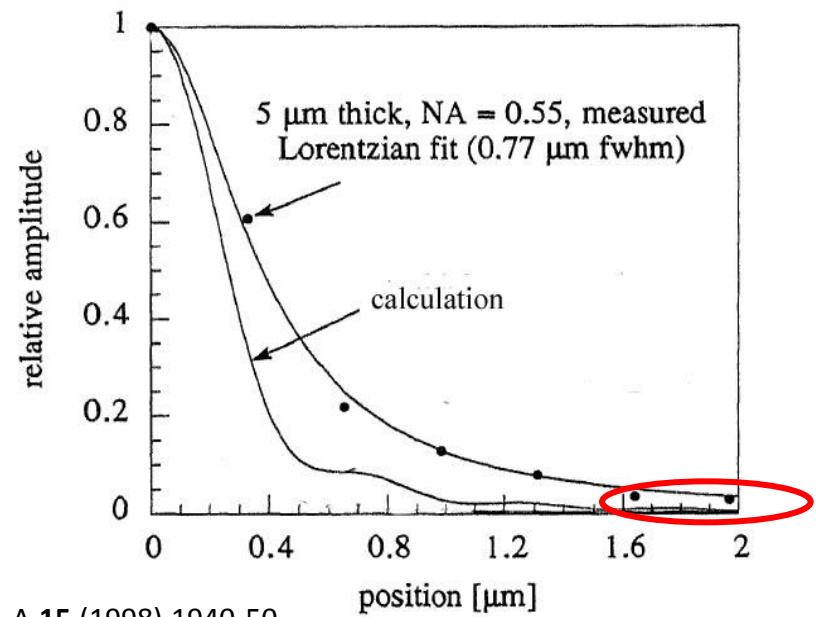
resolution may approach  
optical diffraction limit, i.e.  
 $\sim 0.5\mu\text{m}$  fwhm in 'thin' screen limit  
max' size  $\sim 1\text{cm}$



e.g. doped YAG:Ce by liquid epitaxy on undoped 170 $\mu\text{m}$  YAG substrate,  
X-rays, 100x magnification optics  
CCD 24  $\mu\text{m}$  pixel sampling



Koch et al, J. Opt. Soc. Am. A **15** (1998) 1940-50



65000

16bit

wide range of 'scientific grade' CCD cameras are now commercially available, selected to suit experiment: optimum compromise made between: dynamic range and noise, total pixel count and frame readout speed...

40000

30000

20000

10000

12bit

14bit

Measured dynamic range

0

0.1

1

10

100

10000

1000

100

10

1

0.1

Frelon-Kodak  
2kx2k

Frelon  
Atmel  
2kx2k

PCO.Edge  
Andor Zyla  
Hama Flash 4.0  
2kx2k

Dalsa  
1M60

Sarnoff  
512x512

PCO.Dimax

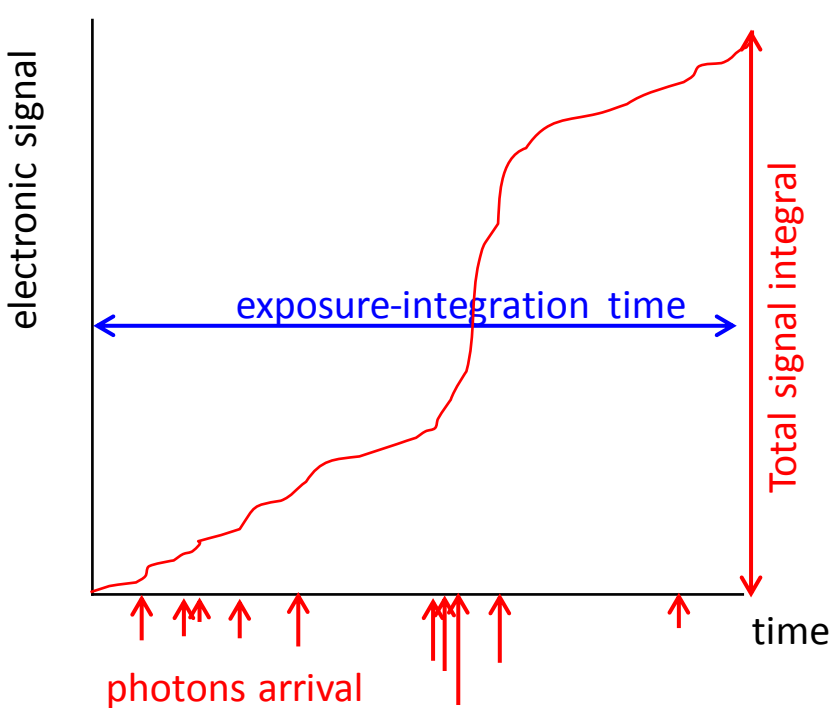
Phantom V1610  
1.3k x 800

Hamamatsu Flash 2.8  
1.9k x 1.4k

Image Readout Frame rate (fps)

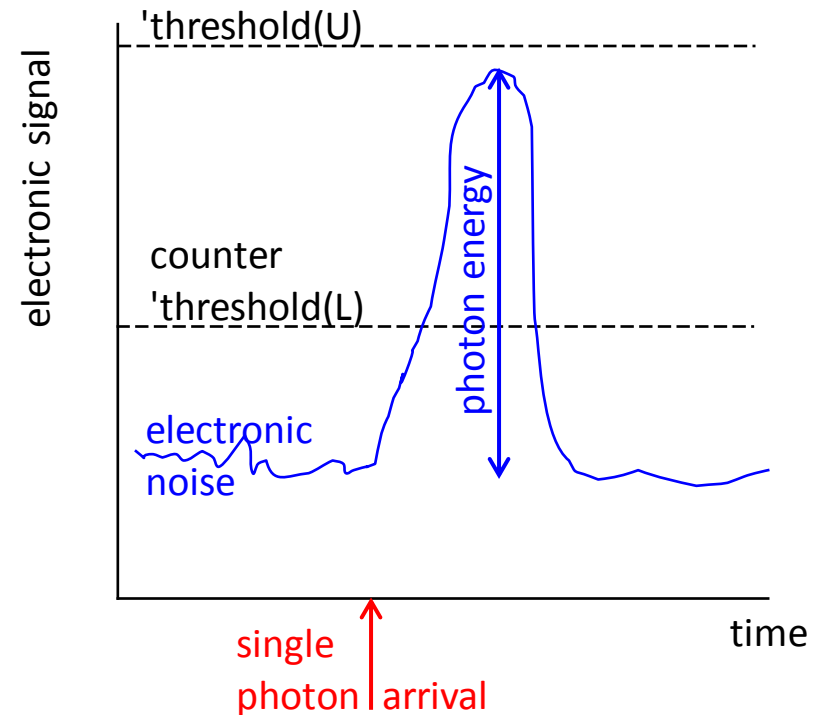
integrating detector:

signal resulting from arrival of (usually)  
many photons is only sampled at the  
end of an 'exposure' period



signal response *remains linear even at very high photon rates,*  
unless detector 'saturates'

energy resolved and counting detectors:  
individual X-ray photons are detected 'one at a time'



*removes detector noise contribution to signal,*  
permits *energy resolved photon detection*  
*...but signal response shows 'count pile-up'*

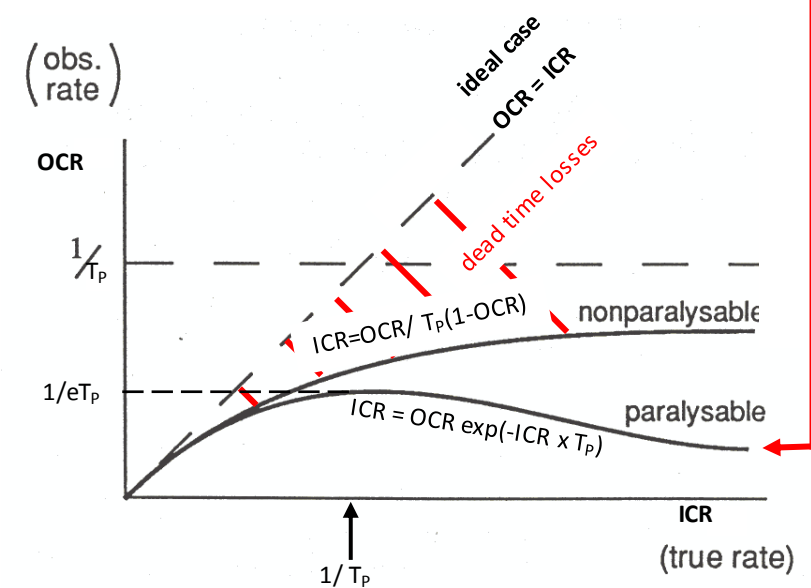
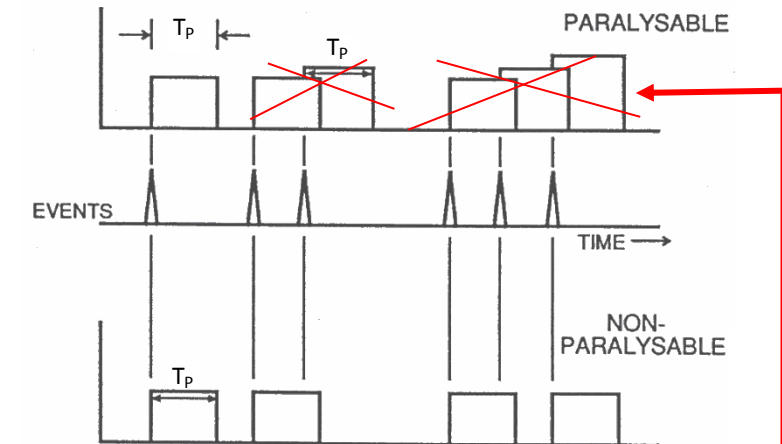
Counting detectors are usually ‘non-paralysable’: two events are counted as a single event if they are separated in time  $< T_p$  the event ‘dead-time’ . Measured count rate response is non-linear, reaching a plateau value for high event rates.

X-ray energy resolving detectors *must be* ‘paralysable’ i.e. time-overlapped pulses must be rejected, else they will be recorded as false events in the measured energy spectrum histogram

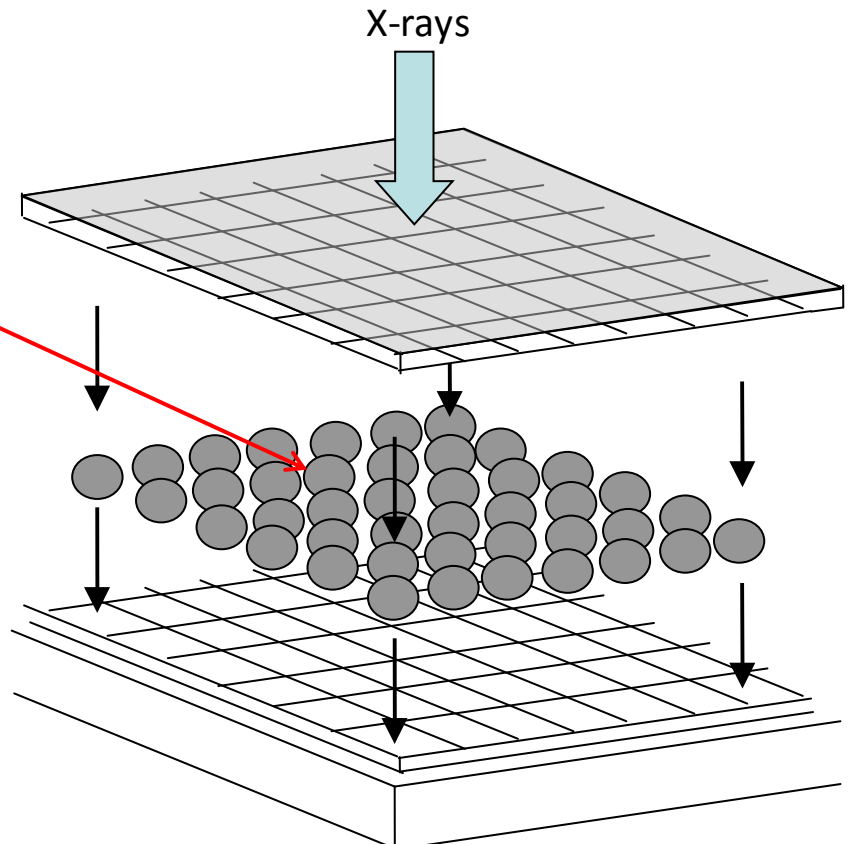
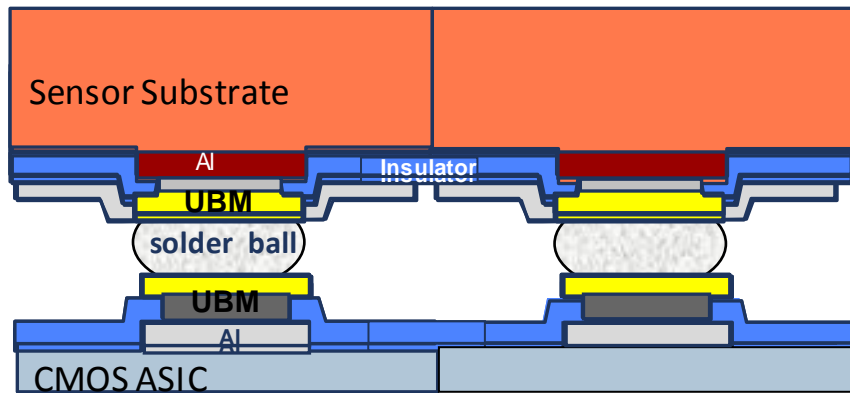
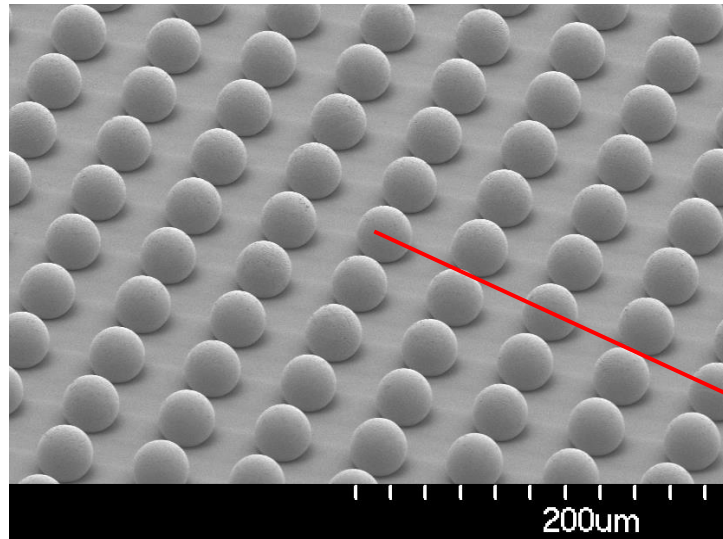
For Poisson time-distributed events, e.g. from a radioactive source, the true input event rate (ICR) at the detector can be obtained from the output spectrum:

$$ICR = OCR \exp(-ICR \times T_p)$$

$T_p \approx 5 \times$  filter ‘shaping time’ of the pulse



*to count faster, use multichannel, parallel-counting 'pixel detector' systems*

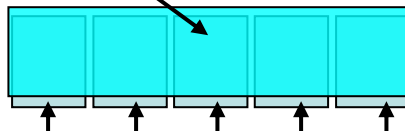


## ESRF 'Maxipix' system, using Cern 'MEDIPIX-2' ASIC and silicon sensor

350 Hz frame rate (5x1 chips) using parallel readout mode  
**55 x 55  $\mu\text{m}^2$  pixel size --high spatial resolution**

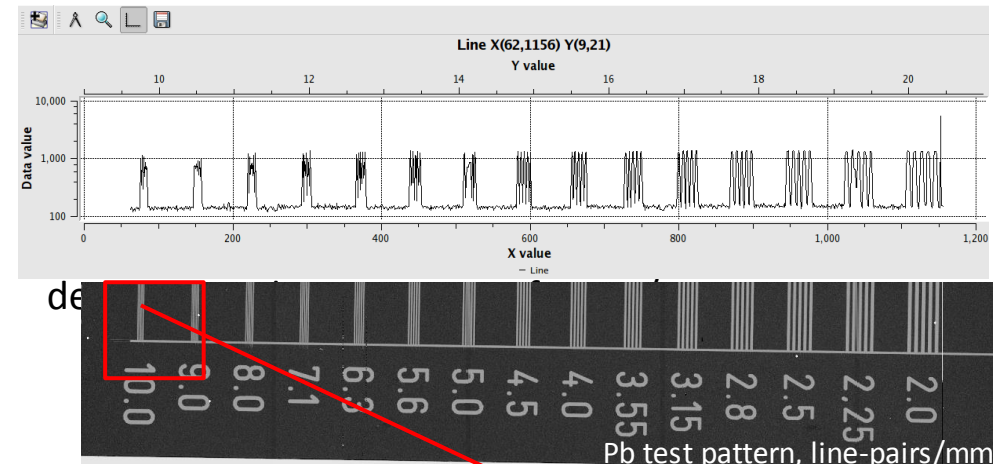


monolithic Si sensor



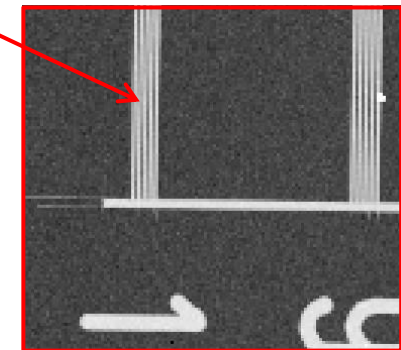
ASIC readout chips

5x1 assembly: 1280 x 256 pixels  
71.2 x 14.1 mm<sup>2</sup> active area

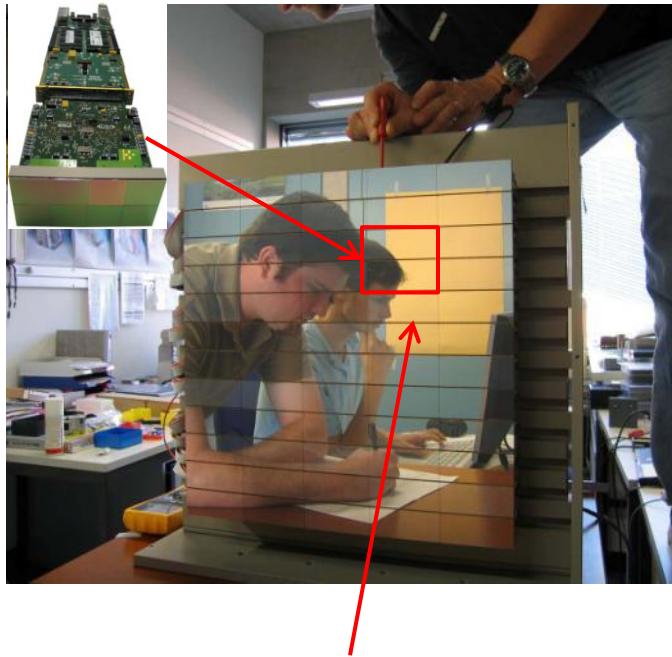


Moiré effect, pixel sampling of spatial frequency close to or below the  
*Nyquist sampling limit = 1/2f*

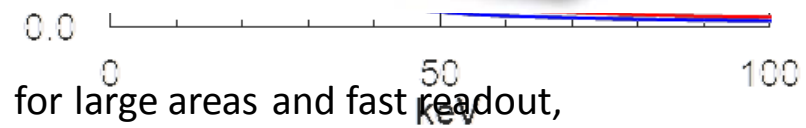
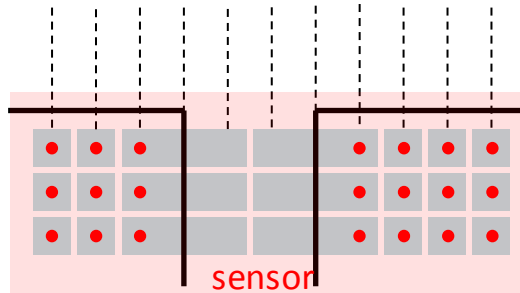
f = spatial modulation frequency of signal



Paul Scherrer Institute developed ASIC (counter) and silicon sensor  
'Pilatus' Systems sold by Dectris Ltd.

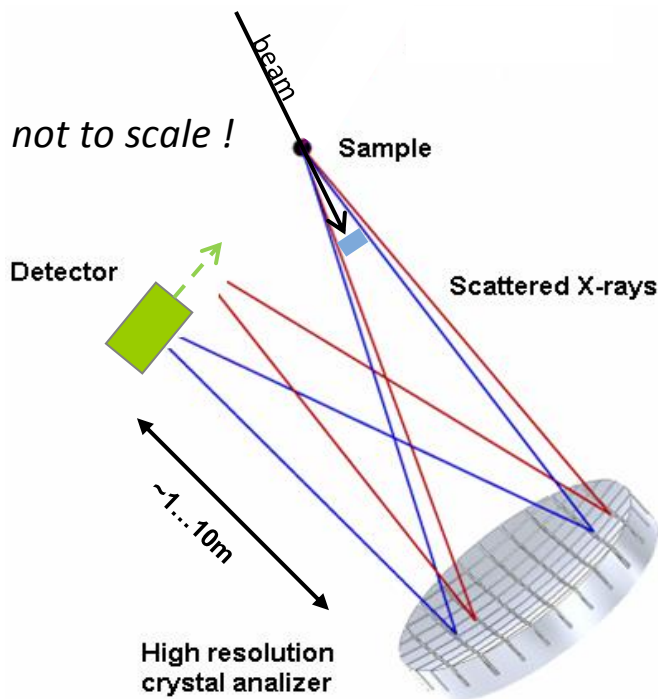


insensitive areas, typically  $\sim 1\text{mm}$  between  
ASICs:



for large areas and fast readout,  
silicon PADs have completely replaced MWPC  
gas detectors at synchrotrons:  
*higher global count rate capacity, reliability ...*

- measurement of 'recoil' energy transferred to the sample by the individual X-ray photons
- energy transfer is small: high energy resolution required:  $1\text{meV} \sim 1\text{eV}$  (e.g. for  $10\text{keV}$  X-rays)
- Use of diffractive crystal *energy analyzer* detection arrangement:



- highly monochromatized beam and weak interaction cross sections  
--> low photon detection rates  
beam on sample  $10^{12}$  photons/sec, but possibly < 1 photon/sec on detector
- use of a position sensitive detector may 'improve' effective energy resolution *and* useful count throughput of crystal analyzer
- detector energy resolution useful to reject stray X-ray background

Possibly measured simultaneously:

- sample absorption
  - sample X-ray fluorescence
- and polarization dependence (e.g. sample *dichroism*)

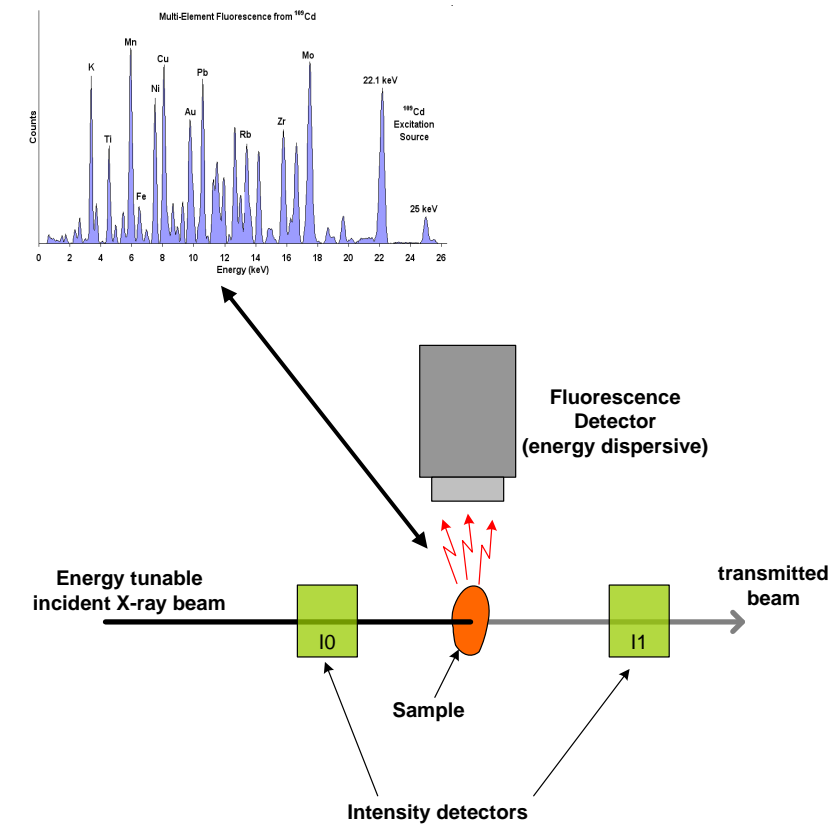
often *measured as function of incident beam energy*,  
sample environment...

detectors:

*for transmitted beam intensity:*  
gas ionization chambers, photodiodes

*for emitted fluorescence:*  
Si, Ge semiconductor detectors

diffractive crystal analysers  
cryogenic bolometers / STJ's



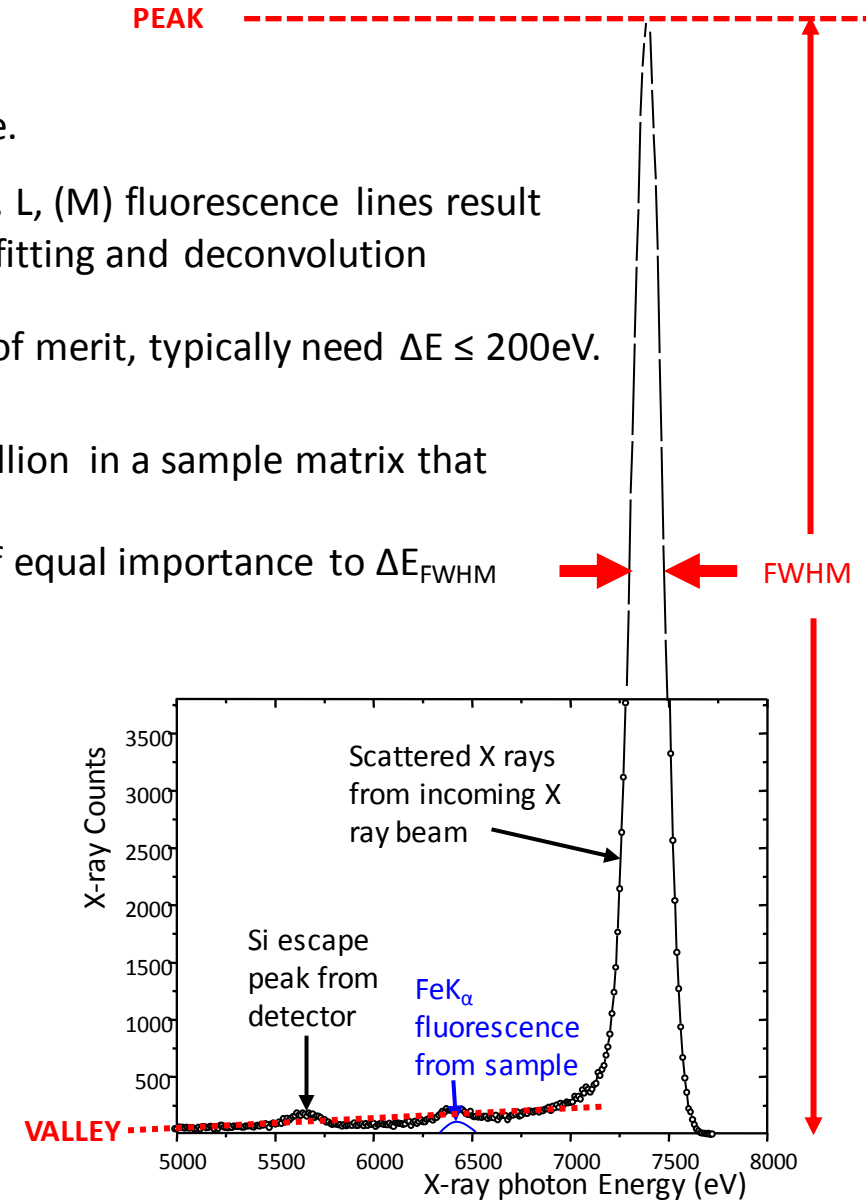
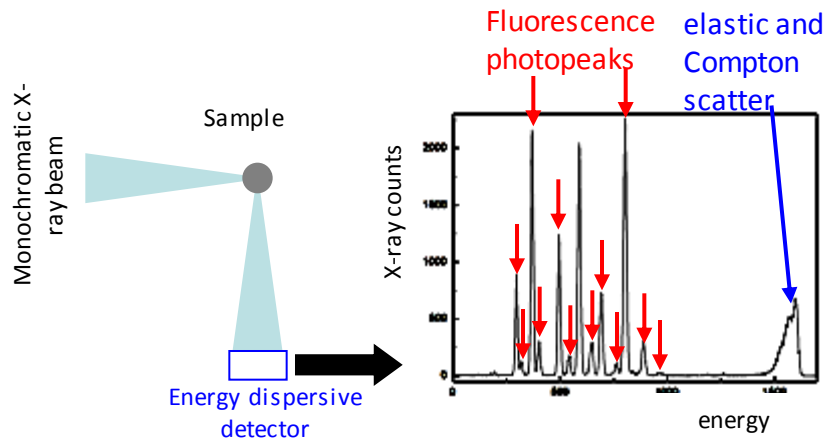
Often need to identify/quantify elements in the sample.

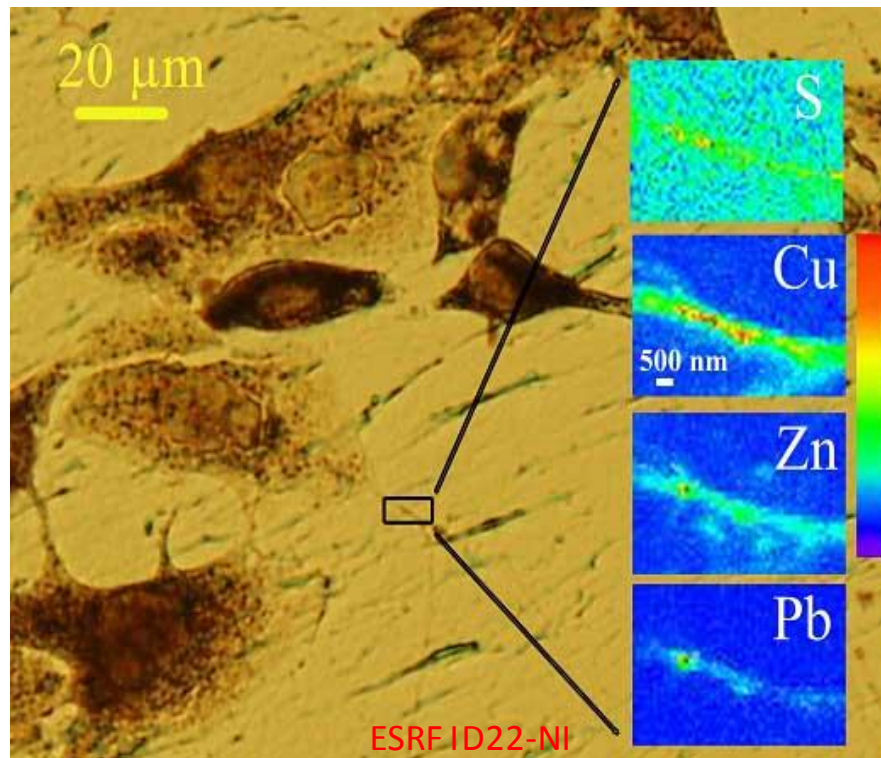
If the sample contains many elements, then multiple K, L, (M) fluorescence lines result in complex energy histograms requiring accurate peak fitting and deconvolution

Energy resolution 'FWHM' is the usual detector figure of merit, typically need  $\Delta E \leq 200\text{eV}$ .

For trace element analysis we may seek < parts per million in a sample matrix that itself fluoresces *and* scatters the incoming beam...

'peak-to-valley' performance of the detector may be of equal importance to  $\Delta E_{\text{FWHM}}$

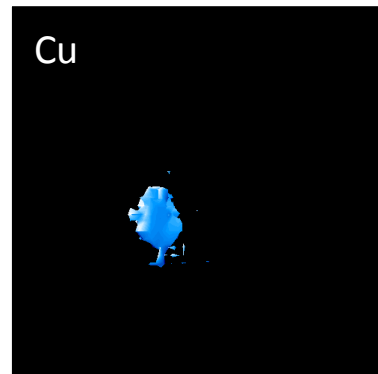
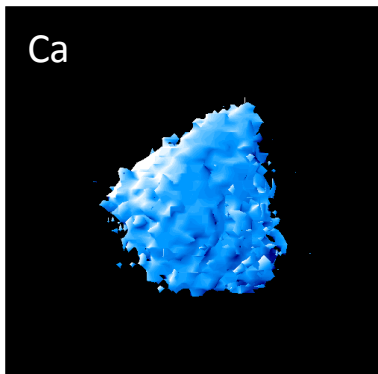
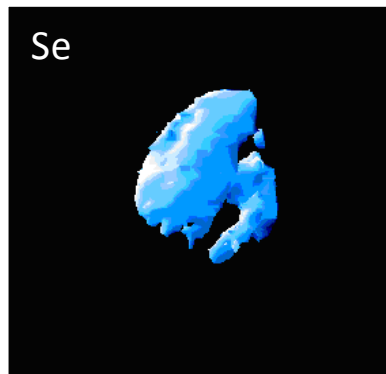
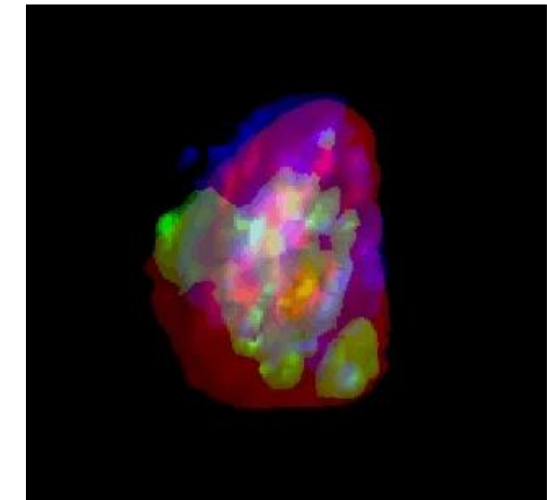
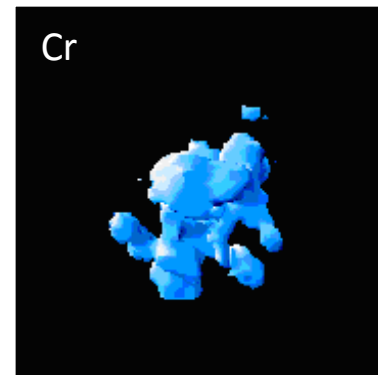
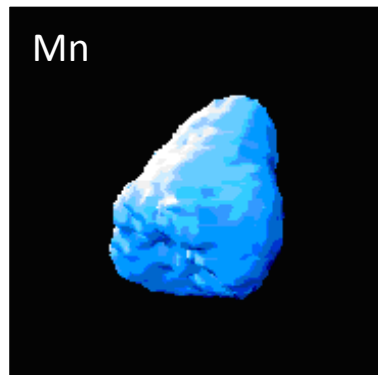
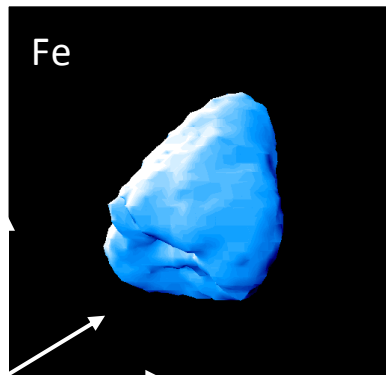




Neurite process  
A Carmona et al.  
JAAS (2008)

Rotation of the sample enables *3D mapping* of element distributions

NASA 'stardust' sample 0044-Track 3/terminal particle: heterogeneous on the submicron level, Fe-rich olivine

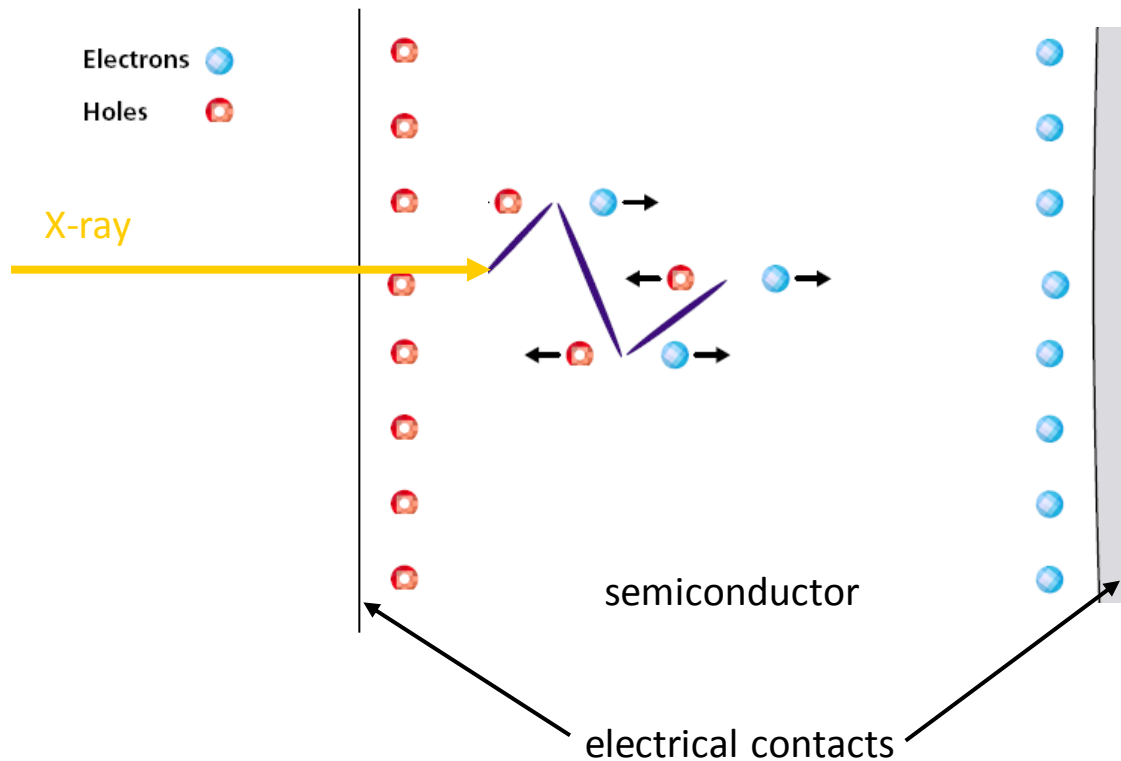


3D tomographic  
reconstruction shows  
distribution of  
*Fe, Cr, Se.*

$\sim 2 \mu\text{m}$

ESRF-ID13', courtesy of Laszlo Vincze, Univ. Ghent

Semiconductor material e.g. high purity silicon with X-ray 'transparent' doped p and n contacts. Applied reverse-bias creates electric field depletes crystal bulk of (thermally generated) charges carriers.



- X-ray interacts (photoelectric absorption or Compton scatter), generates a 'hot' electron which rapidly thermalizes (~psec timescale) creating a cloud of charge .
- charges drift in the electric field towards electrodes over ~nsec to  $\mu$ sec timescale
- electrical signal is developed *while the charge drifts in the bulk... (Ramo, image charge...)*

For a *semiconductor* detector, the *statistical limit* to energy resolution is given by

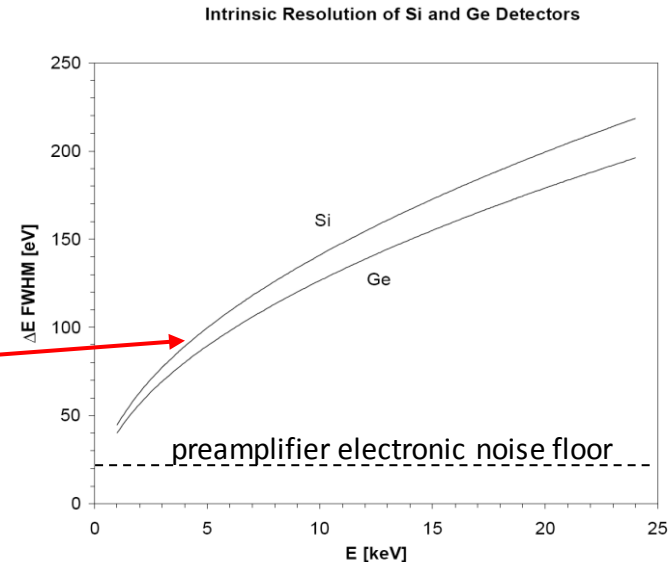
$$\Delta E_{\text{FWHM}} = 2.35 \sqrt{F \epsilon E} \quad \text{where } \epsilon = 3.63 \text{ eV per electron-hole pair for silicon}$$

*Fano factor*  $F \approx 0.11$  for Si and Ge (F is *not* a constant, but can usually be considered as one)

U. Fano, Phys. Rev. 72 (1947) 26

spectral resolution *measured* is the quadrature-sum of the  
**Fano statistics** and **preamplifier electronic noise** contributions:

$$\Delta E_{\text{total}} = \sqrt{(\text{Fano})^2 + (\text{electronic noise})^2}$$



Charge  $q$  created by X-ray absorption is

$$q = 1.6 \times 10^{-19} E_{\text{xray}}(\text{eV})/\epsilon \quad (\text{Coulombs})$$

For a silicon detector with a *charge preamplifier* of feedback  $C_f = 0.1\text{pF}$ , an Xray of 10keV energy gives a voltage- step signal of just 0.4mV, but we need to measure this step with a precision of  $\sim 1\%$  !

*NOISE contribution of the detector preamplifier must be minimized:*

*this is done by reducing measurement bandwidth using an optimized weighting filter*

For a charge preamplifier, the rms ‘Equivalent Noise Charge’ is

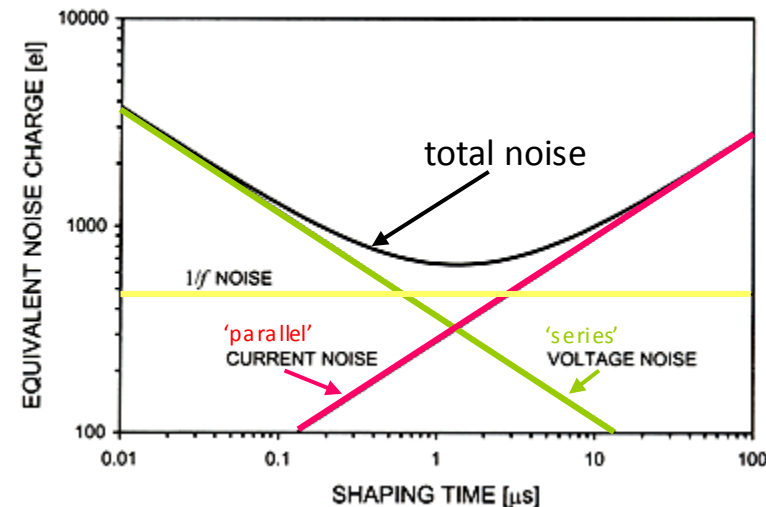
$$ENC \approx \sqrt{\left( \frac{kT}{2R_P} + \frac{eI_D}{4} \right) \tau + \left( \frac{kTC^2}{2g_m} \right) \frac{1}{\tau} + AC^2}$$

parallel noise

series noise

1/f noise

where  $\tau$  is the signal ‘shaping time’ (CR-RC filter)

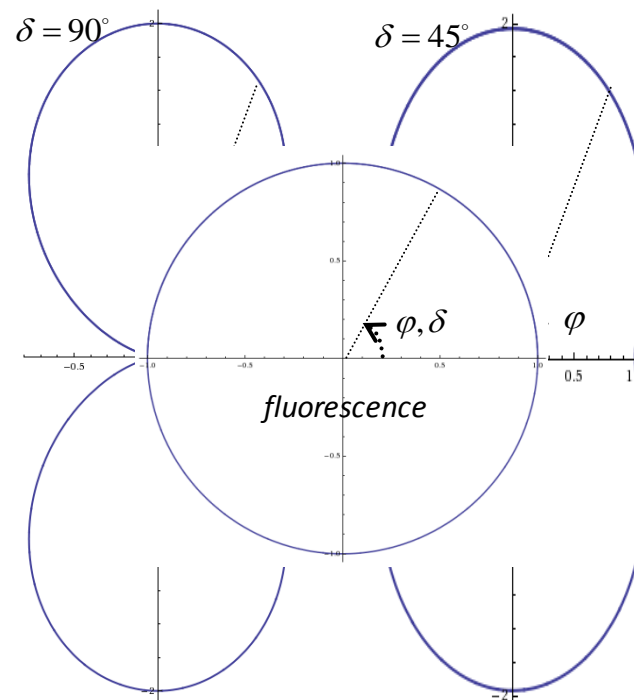
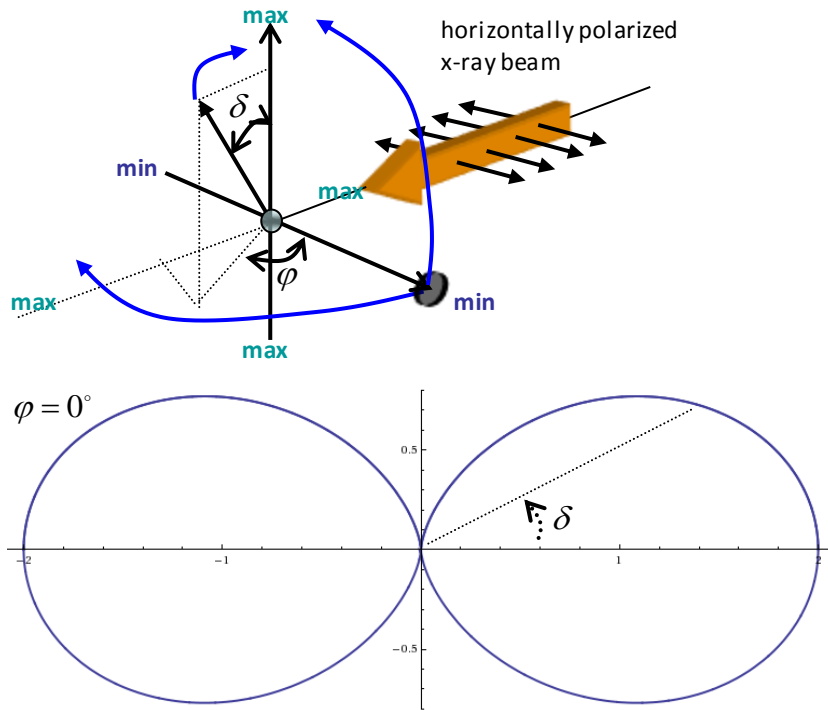


Synchrotron undulator beams focused on the sample are typically  $\sim 99\%$  linear polarized  
 --> strong angular dependence of both Rayleigh (elastic) Compton (inelastic) scattering

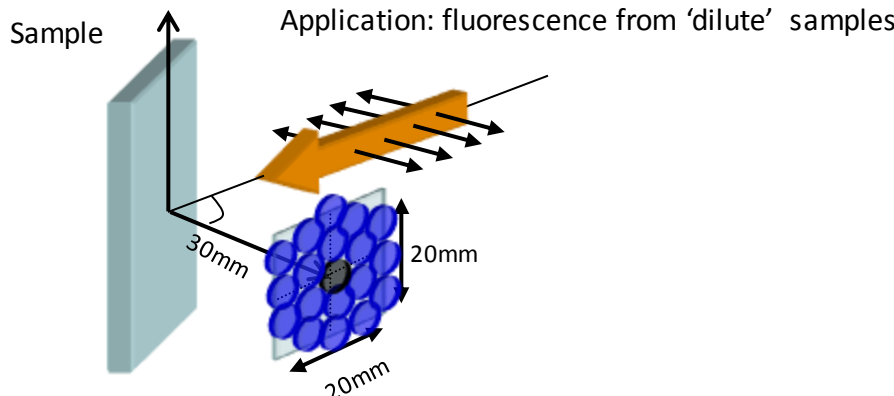
Polarization dependent elastic scattering cross section:

$$\left( \frac{d\sigma}{d\Omega} \right)_{\delta,\varphi} = \frac{r_e}{2} \left( 1 + \sin^2 \delta \cdot \sin^2 \varphi + P_0 [\sin^2 \delta \cdot \cos^2 \varphi - \cos^2 \delta] \right)$$

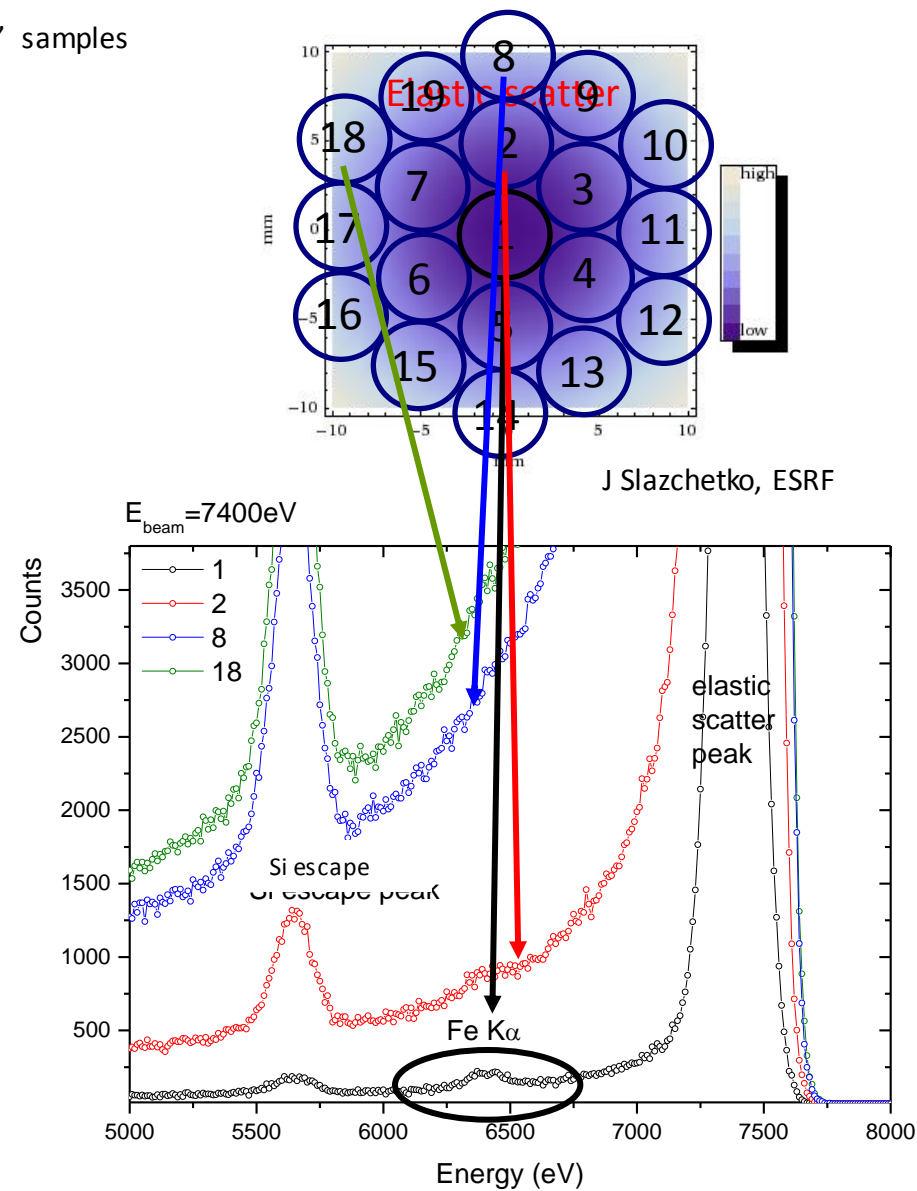
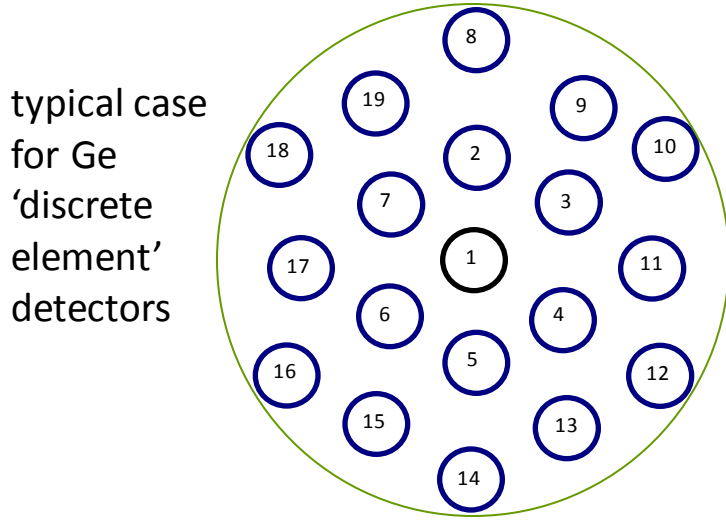
R. E. van Grieken, A. A. Markowicz, Handbook of X-ray Spectrometry (2002).



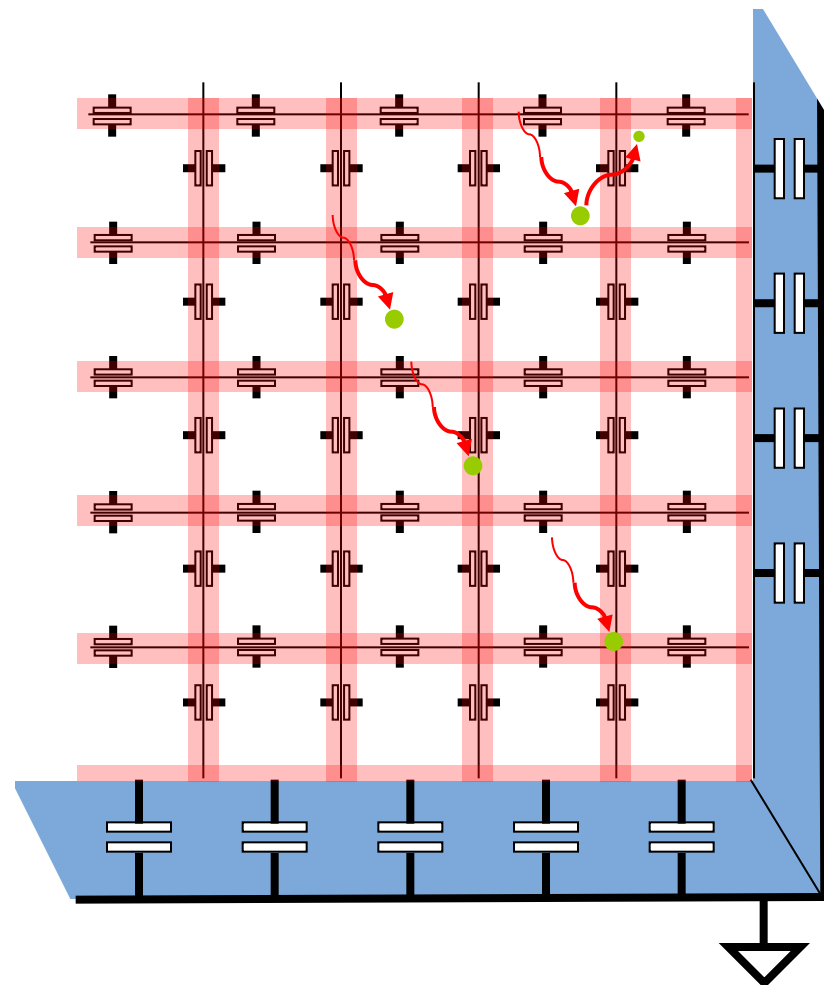
recall that cross section for fluorescence radiation is (almost) isotropic, i.e. independent of  $\varphi, \delta$



→ importance of 'packing factor' of the elements



using lithographic masked doping, a matrix of individual sensing areas can be made on semiconductor detectors. This can give a 100% sensitive area, *but there are challenges*:



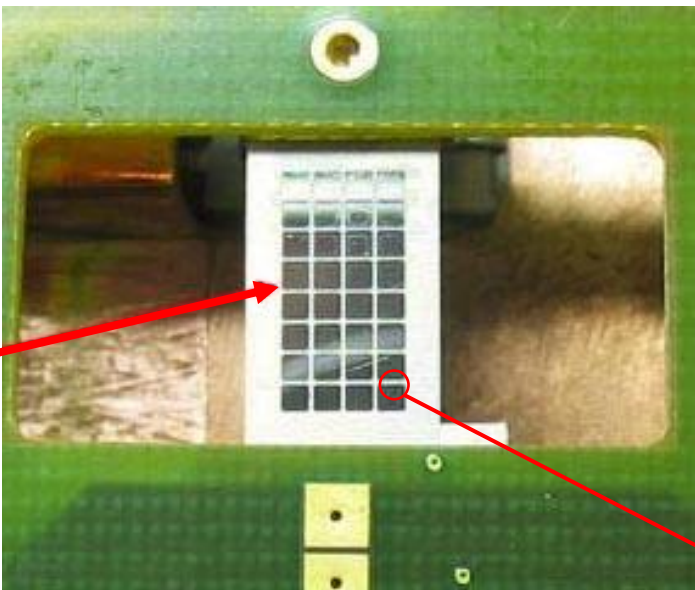
if an X-ray is absorbed near a pixel border, diffusion creates a 'cloud' of electric charge which splits the signal between neighbour pixels

Alternatively, a fluorescence photon may be emitted and absorbed in a neighbour pixel

These *physical crosstalk* effects become more serious as the individual 'pixel' area is reduced. Partial solution is use of a *grid collimator* which hides the pixel edges.

Each sensing area is capacitively coupled to its neighbours: this results in additional *electronic crosstalk*

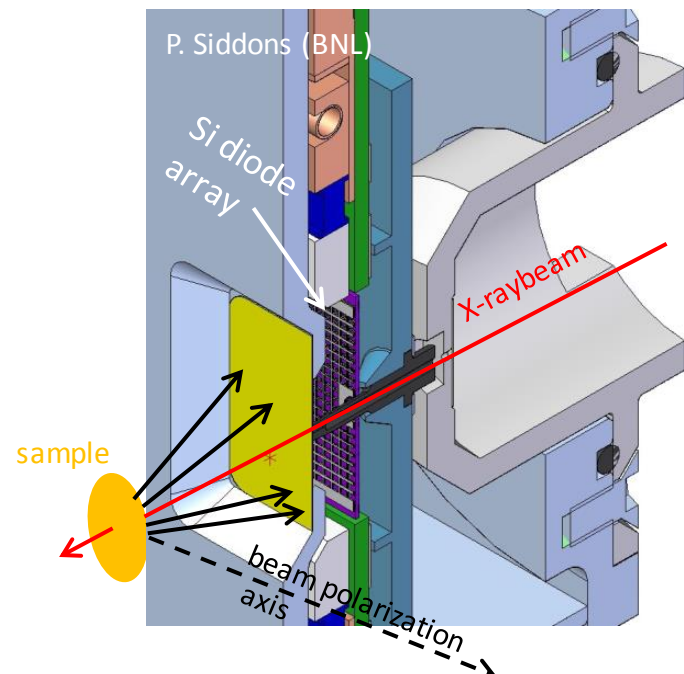
Molybdenum mask on planar silicon detector developed at NSLS-BNL



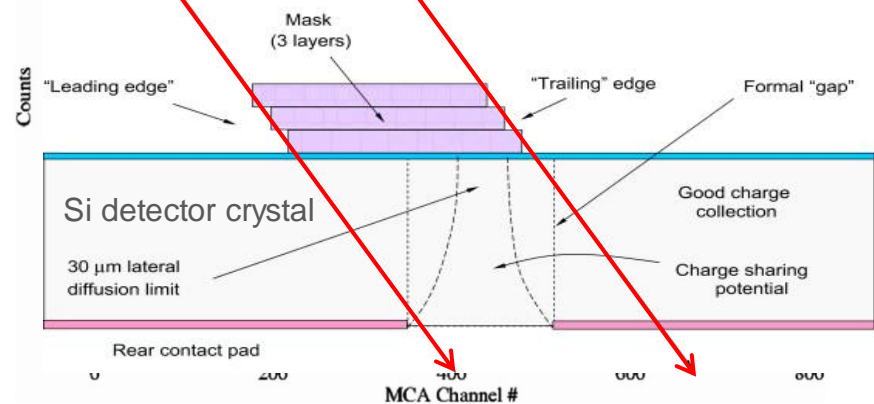
MAIA development: prototype with 32 element pin diode monolithic Si crystal

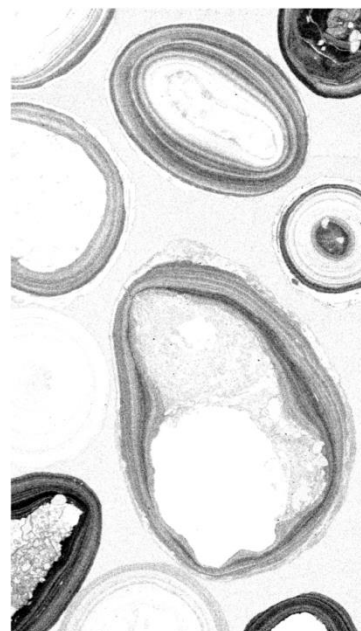
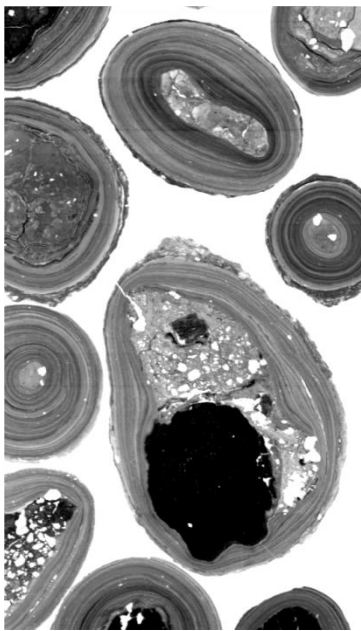
C.G. Ryan et al.

Nucl. Instr. and Meth. Phys. B 260 (2007) 1–7



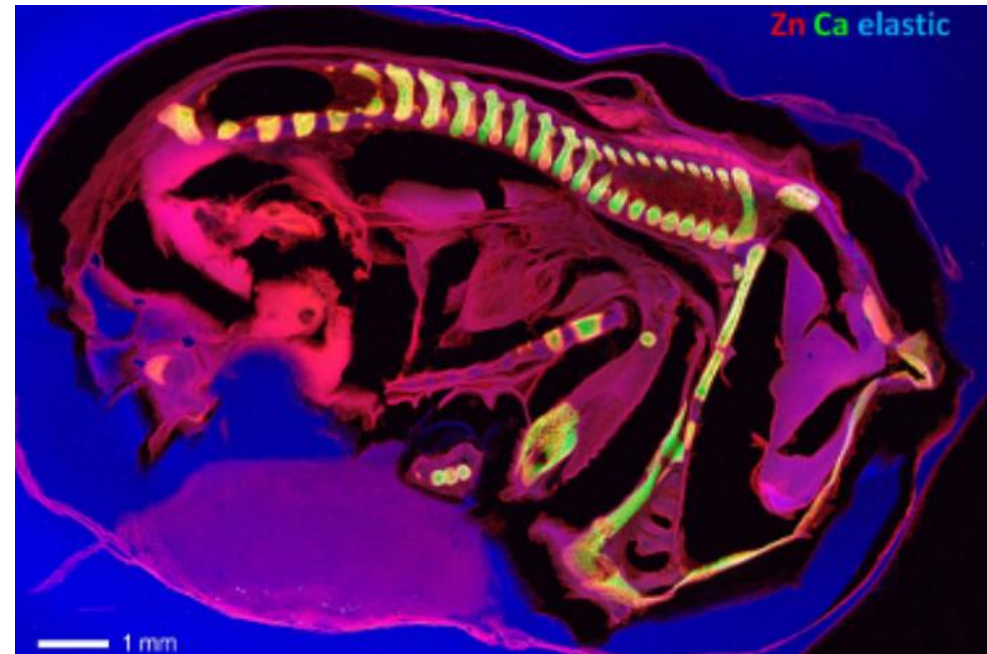
staggered mask, alignment with diode edges  
in final MAIA detector design (384x1mm<sup>2</sup> diodes)





first 96 element MAIA detector: concentrated iron (left) and trace yttrium (right) in iron-oxide nodules: grey scale is element abundance. Sample mapped with 5msec dwell time per 'pixel' position, total of  $1625 \times 2625 \times 7.5\mu\text{m}$  pixels, corresponding to  $13 \times 21 \text{ mm}^2$  scanned area. Beam energy 17.2 keV.

Ryan CSIRO, Siddons BNL et al, 1990

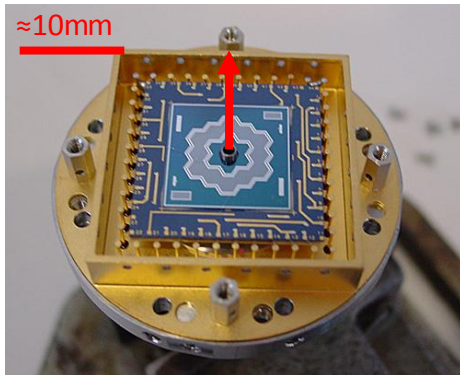
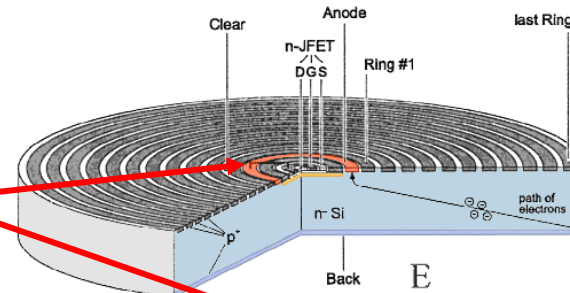


Zn, Ca trace metals in a mouse embryo cross-section image from latest 384 element MAIA detector at the Australian Synchrotron --event detection rates to 10 Mcps  $\rightarrow$  pixel dwell times  $>50\mu\text{s}$  using '*on the fly*' sample motion -data acquisition for 2D mapping the sample; online FPGA based spectrum deconvolution.

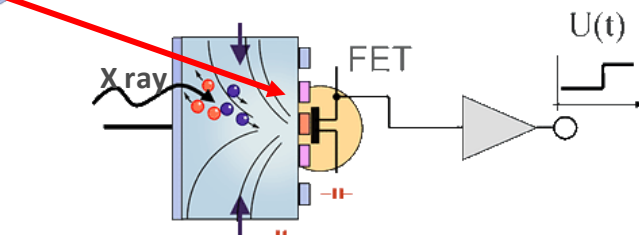
CSIRO website May 2013

Planar silicon technology, multiple electrodes establish transverse drift field , low capacity charge collecting anode / FET  $\sim 100\text{fF}$

preamplifier may be (partly) integrated on detector

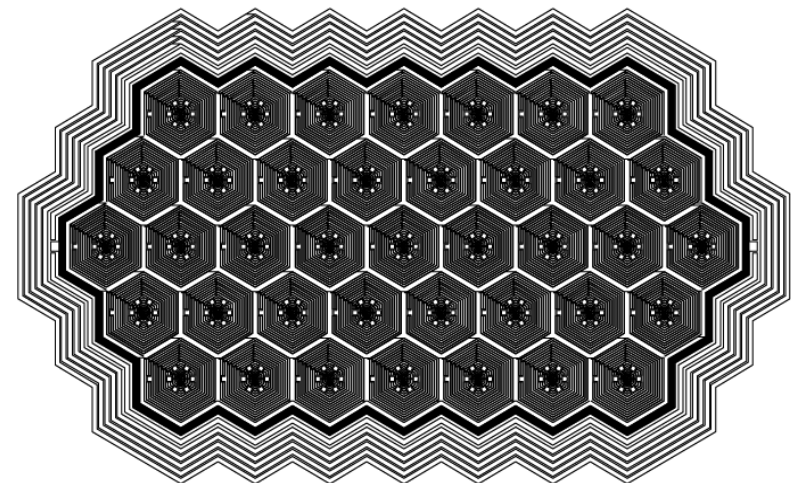


high resistivity silicon  
⇒ low bulk leakage current  
⇒ Peltier cooling usually employed  
 $-10^\circ \dots -50^\circ\text{C}$   
⇒ *compact, lightweight systems, high rate capability  $\sim 1\text{Mcps/channel}$ , with 'Fano limited' energy resolution*



Near wafer-scale lithographic processing  
large, tightly-packed arrays possible  
crosstalk issues

but large cell counts ⇒ yield issues  
⇒ multi channel pulse processors  
⇒ fabrication complexity / cost



39 cell detector with on-chip FETs, total active area  $195\text{mm}^2$  (after Struder, MPI-Garching)

We have presented some of the major detector types used at synchrotron sources and given a basic summary of their operation, but there are *many* other detector types in use, not described here for lack of time.

For many of these 2D (and '3D') detectors, fast data transfer with online visualization and analysis have become major electronic and software engineering challenges.

High performance, high efficiency detectors are as important as the beamline and its X-ray optics:

the X-ray beam intensity can be so high that for many experiments we are limited by the *radiation tolerance limit of the sample*... so we need to make sure that every photon 'counts'.

Fano energy resolution,  
leakage current (noise)

stopping power,  
X-ray absorption length

$$\Delta E \propto \frac{1}{E \sqrt{N}}$$

Signal development time  
(max. counting rate)

Material	Z	Bandgap [eV]	Mobility [cm <sup>2</sup> /Vs]		Density g/cm <sup>3</sup>
			electrons	holes	
Si	14	1.1	1350	480	2.3
Ge	32	0.7	3800	1800	5.3
Diamond	6	5.5	4500	3500	3.5
GaAs	31-33	1.5	8600	400	5.4
AlSb	13-51	1.6	200	700	4.3
GaSe	31-34	2.0	60	250	4.6
CdSe	48-34	1.7	50	50	
CdS	48-16	2.4	300	15	4.8
InP	49-15	1.4	4800	150	
ZnTe	30-52	2.3	350	110	
WSe <sub>2</sub>	74-34	1.4	100	80	
Bil <sub>3</sub>	83-53	1.7	680	20	
Bi <sub>2</sub> S <sub>3</sub>	83-16	1.3	1100	200	6.7
Cs <sub>3</sub> Sb	55-51	1.6	500	10	
Pbl <sub>2</sub>	82-53	2.6	8	2	6.2
Hgl <sub>2</sub>	89-53	2.1	100	4	6.3
CdTe	48-52	1.5	1100	100	6.1
CdZnTe	48-30-52	1.5-2.4			

monoelemental crystals, excellent charge transport

Binary and ternary compounds

Stoichiometry etc

→ trapping of charge during drift

$\mu\tau$  products, schubweg

$\tau_e$ ,  $\tau_h$  carrier lifetimes

Materials already investigated as radiation detectors